Can the tsunami geological record contribute to constrain the tectonic source of the 1755 AD earthquake?

Francisco Dourado[1], Pedro JM Costa[2], SeanPaul La Selle[3], C. Andrade[4], Ana Nobre Silva[5], Ivana Bosnic[5], and Guy Gelfenbaum[3]

[1]Universidade do Estado do Rio de Janeiro
[2]Earth Sciences Department, Faculty of Sciences and Technology, University of Coimbra
[3]United States Geological Survey
[4]Centro de Geologiae Departamento de Geologia da Universidade de Lisboa. Faculdade de Ciencias, Bloco C6, 3degree signPiso,Campo Grande, 1749-016 Lisboa, Portugal
[5]Instituto Dom Luiz, Universidade de Lisboa

November 25, 2022

Abstract

The precise location of the seismic source of Great Lisbon Earthquake is still uncertain. The aim of this work is to use the an onland sedimentary record in southern Portugal to test and validate seismic sources of the AD 1755 earthquake. To achieve this, tsunami deposit thicknesses from over 150 cores retrieved from Salgados (Portugal) were compared to the results of a tsunami sediment transport model (Delft3D-FLOW) which simulates tsunami propagation, inundation, erosion, and deposition. Seven different hypothetical seismic sources and varying bed roughness coefficients were used to determine which modeled sources better reproduce observed patterns of tsunami deposit thicknesses and also dune erosion at the studied site in southern Portugal. Modeled and observed historical tsunami arrival times were also used to test different earthquake sources. Based on these comparisons, four modeled earthquake sources were unable to reproduce the observed physical data, suggesting they should be disregarded as likely sources of the AD 1755 earthquake.

Hosted file

table1_vf.docx available at https://authorea.com/users/528715/articles/605435-can-the-tsunami-geological-record-contribute-to-constrain-the-tectonic-source-of-the-1755-ad-earthquake

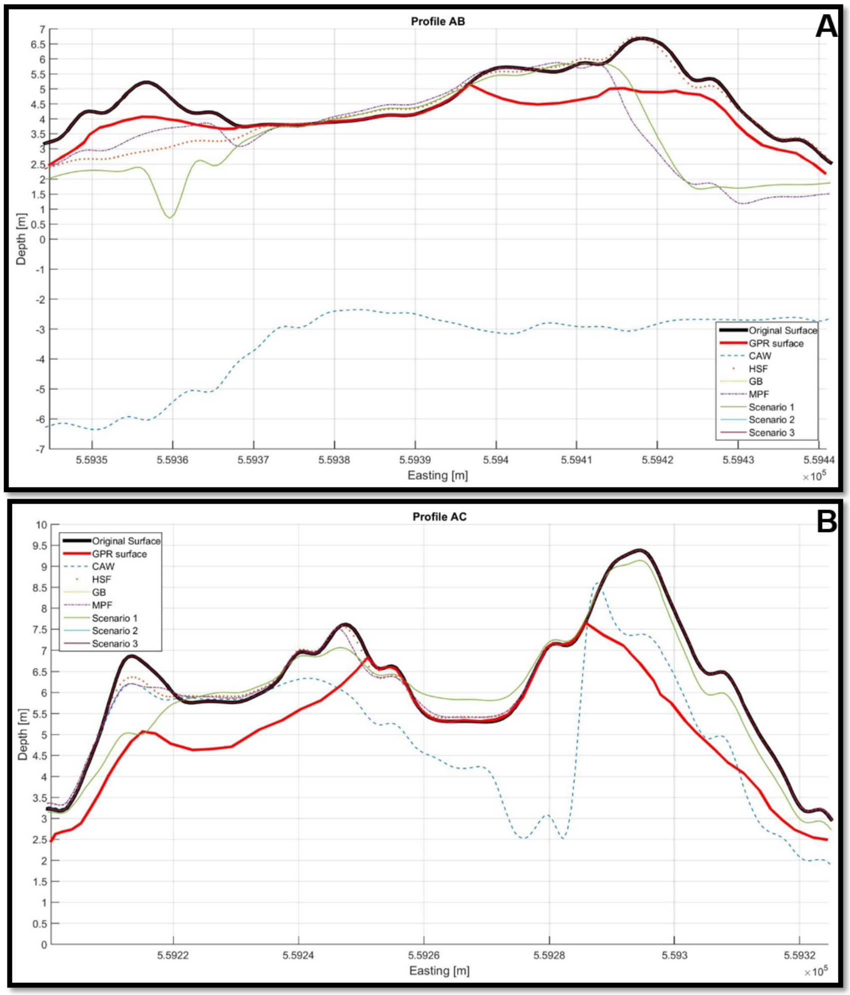
A
Profile AB
Depth [m]
Easting [m]
Original Surface
GPR surface
CAW
HSF
GB
MPF
Scenario 1
Scenario 2
Scenario 3
B
Profile AC
Depth [m]
Easting [m]
Original Surface
GPR surface
CAW
HSF
GB
MPF
Scenario 1
Scenario 2
Scenario 3

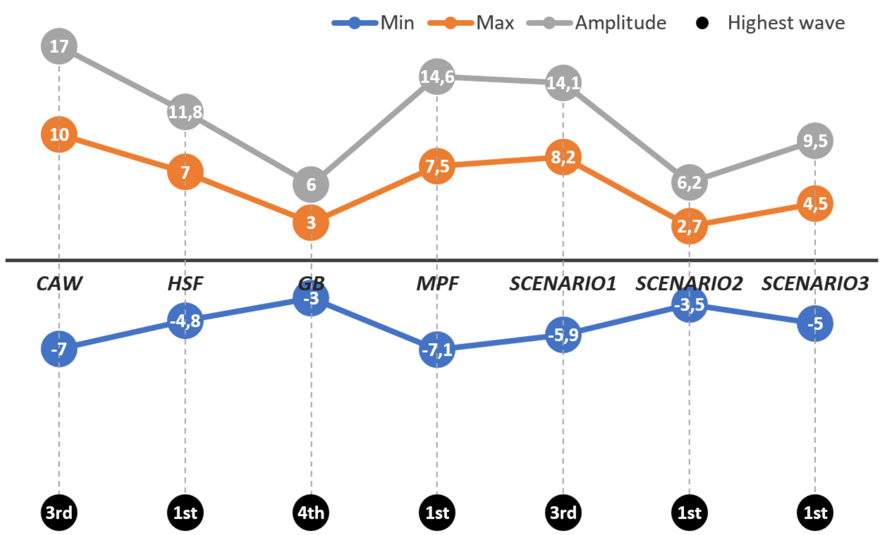
Min
Max
Amplitude
Highest wave
CAW
HSF
GB
MPF
SCENARIO1
SCENARIO2
SCENARIO3
17
11,8
6
14,6
14,1
6,2
9,5
10
7
3
7,5
8,2
2,7
4,5
-7
-4,8
-3
-7,1
-5,9
-3,5
-5
3rd
1st
4th
1st
3rd
1st
1st

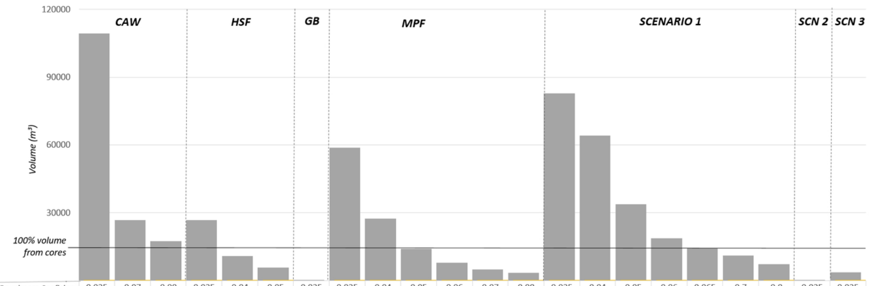

Roughness Coeficient	0.025	0,07	0,08	0.025	0,04	0,05	0.025	0.025	0,04	0,05	0,06	0,07	0,08	0.025	0,04	0,05	0,06	0,065	0,7	0,8	0.025	0.025
Vol. in m³	109400	26800	17400	26700	10867	5831	159	58849	27301	14022	7830	4936	3403	82739	64182	33802	18620	14116	11078	7218	19	3550
% Vol. from cores	762%	187%	121%	186%	75,70%	40,60%	1,10%	410%	190%	97,70%	54,60%	34,40%	23,70%	576%	447%	235%	130%	98,40%	77,20%	50,30%	0,10%	24,70%

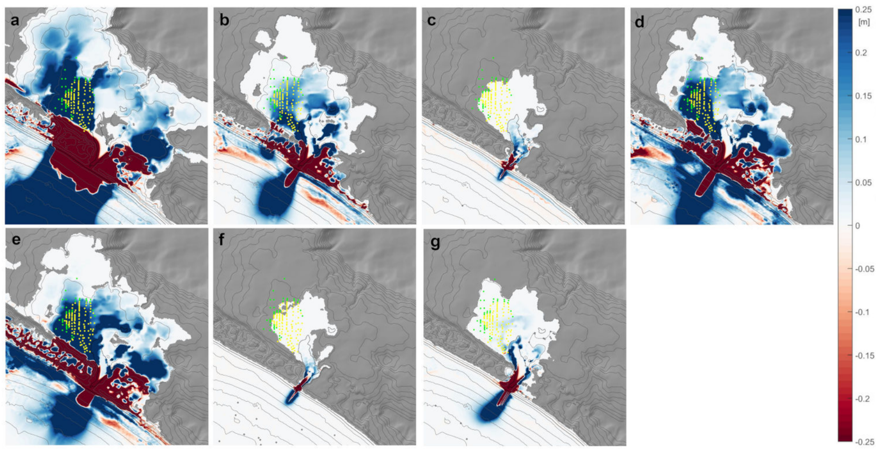

Title

Can the tsunami geological record contribute to constrain the tectonic source of the 1755 AD earthquake?

Authors

Dourado, F., Universidade do Estado do Rio de Janeiro, CEPEDES, Brazil

Costa, P.J.M., Instituto Dom Luiz, Faculdade de Ciências, Universidade de Lisboa, , Universidade de Lisboa, Portugal & Departamento de Ciências da Terra, Faculdade de Ciências e Tecnologia, Universidade de Coimbra, Portugal

LaSelle, S., United States Geological Survey, PCMSC, USA

Andrade, C., Departamento de Geologia, Instituto Dom Luiz, Faculdade de Ciências, Universidade de Lisboa, Portugal

Silva, A.N., Instituto Dom Luiz, Faculdade de Ciências, Universidade de Lisboa, , Portugal

Bosnic, I., Instituto Dom Luiz, Faculdade de Ciências, Universidade de Lisboa, Portugal

Gelfenbaum, G., United States Geological Survey, PCMSC, USA

Abstract

The precise location of the seismic source of Great Lisbon Earthquake is still uncertain. The aim of this work is to use the sedimentary record to test and validate seismic sources of the AD 1755 earthquake. To achieve this, tsunami deposit thicknesses from over 150 cores retrieved from Salgados (Portugal) were compared to the results of a tsunami sediment transport model (Delft3D-FLOW) which simulates tsunami propagation, inundation, erosion, and deposition. Seven different hypothetical seismic sources and varying bed roughness coefficients were used to determine which modeled sources better reproduce observed patterns of tsunami deposit thicknesses and also dune erosion at the studied site in southern Portugal. Modeled and observed historical tsunami arrival times were also used to test different earthquake sources. Based on these comparisons, four modeled earthquake sources were unable to reproduce the observed physical data, suggesting they should be disregarded as likely sources of the AD 1755 earthquake.

Keywords: numerical modelling, Delft3D, sediment transport, sedimentary signatures, tsunami hazard, tsunami sources

1. Introduction

Many different sources have been proposed for the AD 1755 earthquake and tsunami, although to date no single source accounts for the massive energy-release required to: (1) explain the spatial pattern of earthquake intensity observed along the Cadiz Gulf and both the western and southern mainland Portuguese coast, and (2) agree with tsunami travel times observed around and over the Atlantic Ocean. There is no widespread consensus on which specific tectonic structure or structures represent the source of the earthquake and tsunami. Some studies suggest that this event was triggered by interconnected fault or landslide movements (e.g. Vilanova and Fonseca, 2004). Furthermore, the Cadiz Accretionary Wedge (CAW), Horseshoe Fault (HSF), Gorringe Bank (GB) and Marquês de Pombal Fault (MPF) have all been proposed as primary locations where fault-rupture might have generated the AD 1755 earthquake (Wronna et al. 2015; Baptista et al. 2011; Omira et al. 2009; Ramalho et al. 2018; Lima et al. 2010; Baptista et al. 2003; Barkan et al. 2009; Gutscher et al. 2006; Gjevik et al. 1997; Baptista et al. 1998) (Figure 1).

Most of the studies that identify specific sources for the AD 1755 earthquake primarily utilize data derived from reports compiled on Arquivos do Ministério do Reino (1756), which contains information on the locations and times when ground shaking was felt, in addition to reports of damage (Santos and Koshimura 2015; Baptista et al. 1998). Other studies were based exclusively on simulations of tsunami travel times, either from proposed earthquake sources to the locations where observed data describes the time of arrival and impacts of tsunami waves (Gjevik et al., 1997), or by using target-to-source back-ray tracing (Baptista et al., 1996; Baptista et al., 1998). However, no single triggering mechanism proposed so far has been able to reproduce all of the tsunami travel times inferred from the historical records.

Our approach initially models tsunami propagation from proposed seismic source-areas (initial boundary conditions) to selected coastal target-locations. Secondly, travel times are derived and validated with the documentary data. Finally, we model patterns of onshore inundation including inland sediment transport and effects on coastal morphology at Salgados lowland (Figure 1). This coastal lowland contains high-resolution geological and geomorphological datasets that provide objective information on deposition and erosion induced by the AD 1755 Lisbon tsunami (Costa et al., 2012). This allows for rigorously testing a number of proposed earthquake and tsunami sources by expanding the number and diversity of metrics used as validation criteria.

2. Geologic evidence of the AD 1755 tsunami in the Salgados lowland

In this study we use a geological dataset consisting of data from over 150 cores obtained at the Salgados coastal lowland, Portugal (Figure 1). The lowland corresponds to a sediment-choked lagoon separated from the ocean by a sand beach backed by a multiple-ridged dune. Landward of the dune, the AD 1755 tsunami deposit has been characterized as a massive to normally-graded, sheet of marine-facies shell-rich sand with an erosive base sandwiched in lagoonal mud (Costa et al. 2012; Costa et al. 2016). The tsunami deposit is roughly 50 cm thick closer to the sea and thins in both landward and alongshore directions (Figure 1). Costa et al. (2012), Costa et al. (2016) and Moreira et al. (2017) used paleoecological, geochemical, mineralogical, microtextural and grain-size data from tsunami and modern surface sediments from Salgados lowlands to show that the primary source of the tsunami sediments were the dunes and secondarily the beach.

Costa et al. (2016) present data from a Ground Penetrating Radar (GPR) investigation of the dunes at Salgados. Two cross-shore profiles (AB and AC in Figure 1) extending from the upper beach towards the backbarrier area provided information on the architecture of the dune complex, sediment packages and erosional features. Profile AB is 210 meters long and located 300 meters to the west of the Salgados inlet channel, where the dune crest reaches 8.5 m MSL (Figure 1). Profile AC is 245 meters long and is located 120 meters westward of AB. Profile AB presents a dune crest that reaches 11 m above MSL. Both profiles contain a clear image of an erosional surface within the dunes at approximately 6m above MSL. Optically Stimulated Luminescence

(OSL) dating of dune sands immediately below and above that surface constrained an episode of erosion to the mid-17th century (Costa et al. 2016). Regional tsunami historical records, however, suggest that wave heights at the coast were higher, up to 12 m above MSL (Costa et al. 2016).

3. Tsunami modeling methods

To validate tsunami hydrodynamic and sediment transport models we tested 7 different hypothetical fault (source) areas for the AD 1755 earthquake. All source areas considered herein have been previously proposed in the literature and include the Marquês de Pombal Fault (Baptista et al. 2003; Omira et al. 2009; Wronna et al. 2015; Lima et al. 2010), Gorringe Bank (Gjevik et al. 1997; Baptista et al. 2003; Omira et al. 2009; Wronna et al. 2015), Cadiz Accretionary Wedge (Gutscher 2006;Omira et al. 2009; Lima et al. 2010; Wronna et al. 2015; Ramalho et al. 2018;), Horseshoe Fault (Baptista et al. 2003; Barkan et al. 2009; Omira et al. 2009; Lima et al. 2010; Baptista et al. 2011; Wronna et al. 2015; Ramalho et al. 2018) and 3 new hypothetical composite scenarios combining some of these shallow faults with deeper (30-60 km) ones (Figure 1, Table 1).

The initial sea surface perturbation generated by the sources considered has been computed using Mansinha and Smiley (1971) elastic deformation approach through Mirone software (Luis, 2007). The first four sources represent uniform slip on faults: Cadiz Accretionary Wedge (CAW), Horseshoe Fault (HSF), Gorringe Bank (GB) and Marquês de Pombal Fault (MPF). Parameters for these sources were derived from previous studies that validated sources against historically observed tsunami arrival times and ray-tracing, but not against the geological record.

The next three hypothetical sources, Scenarios 1, 2 and 3, are three rearrangements of the 1969 Lisbon earthquake source (Fukao 1973) and a possible combination with a seismogenic structure located between GB and HSF at about 30-60 km deep (Silva 2017). Scenario 1 results from a simple combination of the GB and HSF sources. In Scenario 2 a fault crosses the GB and HSF, while in Scenario 3 it is limited by these. In scenarios 2 and 3 are located at 60 km depth.

Tsunami propagation, inundation, and sediment transport were modeled using Delft3D-FLOW, which solves the nonlinear shallow water equations using a finite difference scheme and has been validated against analytical, laboratory, and field measurements of tsunami hydrodynamics (Apotsos et al., 2011). Three nested grids were prepared with spatial resolutions of 232 m (Level 0), 100 m (Level 1), 50 m, 25 m, and 5 m (Level 2 - varying spatial resolutions on a single grid). Also a synthetic tide gauge was added 500 m offshore southward of Salgados near the 10 m isobath to monitor tsunami water levels (Figure 1).

A combined bathymetric-topographic DEM was created from three different datasets with vertical datum adjusted to MSL at the Cascais tide gauge, 25km west of Lisbon. The DEM was adjusted by using lithostratigraphic data from the 150 sediment cores retrieved from the lowland to reconstruct the approximate surface prior to the AD 1755 event. A final correction of -1.5 m was applied to the DEM to account for the rising tide observed at the time of the earthquake.

A depth-averaged (2DH) model was run using the weakly reflective Riemann boundaries on all grid levels in order to calculate tsunami-induced hydrodynamics. Run-ups (i.e. height reached on the observation points) and tsunami travel times were compared to observations at 4 sites (Sines, Cabo de São Vicente, Lagos and Huelva) (Figure 1). Sediment transport in Salgados was calculated by running the model within Level 2 grid with 10 vertical sigma layers (3DV) in order to resolve important sediment dynamics near the bottom. An unlimited erodible sediment source is represented in the model as a 10-15 m thick sand extending from the offshore to the back of the foredune, with no sand available in the muddy lowland area. In all simulations, the median grain size sediment parameter [D50] used was 250 µm with a density 2,650 kg/m^3. In order to test the sensitivity of model outputs regarding bed roughness, we adjusted the Manning's n roughness coefficient between 0.025 to 0.080 in the dune and lowland areas.

4. Model results

Comparison between the historical data for the arrival times at Sines, Cabo de São Vicente, Lagos and Huelva and modeled results is presented in Table 1. These results indicate that the best overall match between documentary data and modeled arrival times were obtained using the MPF and HSF sources, which yielded lower mean errors (less than 3% and 4% respectively) than other sources The worst correlation corresponds to CAW and GB sources with mean errors of 23% and 28%, respectively. In contrast, the modeled and observed tsunami run-up values at Cabo de São Vicente and Lagos are in excellent agreement for the CAW source (Table 1). The mean errors for run-up results found in relation to other sources were: HSF - 18%, MPF - 10%, Scenario 1 - 21%, GB - 39%, Scenario 2 - 47% and Scenario 3 - 52%.

Sediment transport simulations for GB, Scenario 2 and Scenario 3 sources, using a conservative low bed roughness of 0.025, were not able to reproduce a tsunami deposit volume of more than 25% of the measured volume in Salgados (Figure 2, 3 and 4). The modeled volumes from the CAW and Scenario 1 sources reach or exceed 100% of the measured volume over a range of bed roughness values ranging from 0.025 to 0.065. Using a Manning's roughness coefficient of 0.080 with the CAW source, the simulated volume of sediment deposited was 121% of the volume calculated from CS (Figure 2). Results for all sources using a Manning's n value of 0.025 for the entire domain are shown in Figure 4. The effects of varying the value of Manning's roughness coefficient from 0.035 to 0.065 in the spatial distribution of modeled erosion and accumulation at Salgados for HSF, MPF and Scenario 1 sources, are shown in Figure 4. Erosion on southwest and northeast flanks on the dunes along profiles AB and AC (Figure 5) was reasonably well reproduced using CAW, HSF, MPF and Scenario 1 sources. It is noteworthy that the CAW source overestimates erosion, in contrast with the HSF solution, that clearly underestimates in erosion in both intensity and spatial extent when compared to GPR profile data (Costa, 2016). Results for simulations related to GB, Scenario 2 and Scenario 3 sources fail to fully reproduce this erosional pattern. Comparison between modeled inland extent and depositional signature is difficult because there is an intrinsic underestimation in this approach.

4.1 Gorringe Bank, Scenarios 2 and 3

Our results allow to disregard the hypothetical Scenarios 2 and 3 and the Gorringe Bank as probable sources, because the modeled tsunami waves were far too small to generate significant inundation and consequently unable to produce a tsunami deposit. Compared to historical observations, the modeled run-ups were smaller and the modeled tsunami travel time from Gorringe Bank (GB) was too large. Travel times for Scenarios 2 and 3 tsunami travel time displayed a good fit in the impacted areas near the source, but were too long in sites farther afield.

4.2 Cadiz Accretionary Wedge

For the Cadiz (CAW) source, the modeled run-up agrees well with the historical data. However, the modeled tsunami travel time is shorter than indicated in the historical documents (i.e. modeled tsunami waves travelled app. 20% slower). Furthermore, the modeled sediment deposit volume is eight times larger than the volume calculated from geological data retrieved from cores. In order to achieve an erosion depth compatible with the GPR (cross-dune) profiles described by Costa et al. (2016) it is necessary to use an unrealistical high roughness coefficient (> 0.08) that is not in agreement with the land cover observed in the Salgados lowland (Chow 1959). Furthermore, the resulting (modeled) deposition/erosion profile does not agree well with field data described in Costa et al. (2016).

4.3 Horseshoe Fault

The Horseshoe Fault (HF) model results do not agree well with the observed data. The modeled tsunami arrives 4 minutes later in Sines than in the historical record. Likewise, the modeled run-up for Cabo de São Vicente was 5 meters higher than reported in historical records. The modeled sediment volumes deposited in the lowland are compatible with objective observations when using Manning's n coefficient values between 0.025 and 0.040, which are in broad agreement with the land cover. The model predicted larger amounts of erosion than observed on the seaward section of the dune along profile AB, and less erosion on the landward section. On profile AC, the model predicted no erosion.

4.4 Marquês de Pombal Fault

Both modeled tsunami travel times and run-up magnitude correlate well with the observed historical data. There is also a close correspondence between the observed and modeled volume of the tsunami deposit when using a realistic Manning's n coefficient of 0.04 to 0.05. However, the modeled dune erosion only partially matches the GPR data. Actually, the model fails to correctly reproduce erosion along profile AC on the landward region of the dune, possibly because the largest simulated wave could not overtop the dune obstacle; this obstructed representation of flow along its landward slope and computation of the corresponding erosion.

4.5 Scenario 1

Simulated tsunami travel times obtained from this setting yields good results in all target locations with the exception of Sines and Cabo São Vicente, where simulated travel times are higher. Furthermore, the modeled run-up is approximately 20% higher than reported in the historical records. However, it is noteworthy that the modeled patterns of dune erosion and the volume of sediment deposited in the lowland predicted by the models correlate well field data when a relatively high Manning roughness coefficient of 0.060-0.070 is used.

5. Discussion and Conclusions

The geological record of the 1755 tsunami provides an independent dataset able to validate tsunami propagation and sediment transport models and to test hypothetical earthquake sources. Among the seven hypothetical scenarios presented above, the Marquês de Pombal (and Scenario 1) provide the best overall match with both source-to-target tsunami travel time and run-up taken from the documentary record sources. In addition, they also provide the best overall match in terms of predicted erosion/deposition patterns (e.g. total volume) obtained from field (geological evidences).

The source closest to shore (Marquês de Pombal) yielded the best correlations between modelled and field data. This suggests the region southwest of Cabo São Vicente as the most likely epicenter of the AD 1755 earthquake. This has been previously proposed by Baptista et al. (1992) based on the location of the February 1969 earthquake and also based on back-ray tracing (Baptista et al., 1998). In contrast, all simulated sources located further south in the Cadiz region (CAW and Scenario 1) over-predict the volume of the tsunami deposit in Salgados lowland, the magnitude of run-up reported in the documentary record, thus suggesting that a Cadiz Accretionary Wedge source model is an highly unlikely source of the AD 1755.

Although the Gorringe Bank source has been favored by Santos and Koshimura (2015), its use in the context described herein leads to unacceptable mismatch with both sedimentary and hydrodynamic results as well as with the documentary record in terms of travel time and run-up. In fact, it presented the poorest overall agreement results among all tested sources. This was mainly due to the large distance travelled by the tsunami waves (> 200 km) before impacting the coast. Tsunami travel times and run-up inferred from this source were consistently longer and smaller, respectively, when compared with field and historical data. Scenarios 2 and 3 characterize a deeper source that, according to the modeled results presented in this work, would be incapable of generating a tsunami with similar impact to the AD 1755.

The numerical modeling approach carried out on this work provides an innovative methodology where the robust geological record was able to partially constrain proposed AD 1755 earthquake source hypothesis. It is important to stress that this exercise does not unequivocally resolves the age-old question about the AD 1755 epicenter, nevertheless it points future directions for other fields of geoscience to pursue and, hopefully, it will contribute to the establishment of more reliable hazard assessments for Iberia and for the mid-North Atlantic.

Acknowledgments

The authors thank the Fulbright Commission for Junior Faculty Member Award (2018) for the financial support, the Pacific Coastal and Marine Science Center/United State Geological Survey (USGS), the Foundation for Research Support of the Rio de Janeiro State (FAPERJ) for a Young Scientist of Our State Grant (2016). Authors would also like to acknowledge FCT funded project OnOff - Coupling onshore and offshore tsunami record: complementary tools for a broader perspective on tsunami events - PTDC/CTA- GEO/28941/2017. The authors confirm that the data supporting the findings of this study are available within the article and on a public open database 4TU.ResearchData with the DOI: 10.4121/uuid:99cf3b07-43e4-4a3b-986b-835811aad485

References

Apotsos, A., Gelfenbaum, G., Jaffe, B., Watt, S., Peck, B., Buckley, M., & Stevens, A. (2011). Tsunami inundation and sediment transport in a sediment-limited embayment on American Samoa. *Earth-Science Reviews*, *107*(1–2), 1–11. https://doi.org/10.1016/j.earscirev.2010.11.001

Apotsos, A., Jaffe, B., & Gelfenbaum, G. (2011). Wave characteristic and morphologic effects on the onshore hydrodynamic response of tsunamis. *Coastal Engineering*, *58*(11), 1034–1048.

Arquivos do Ministério do Reino, . (1756). *Inquérito do Marquez de Pombal (Maço No. 638)*. Lisbon, Portugal: Arquivo Nacional da Torre do Tombo.

Baptista, Maria Ana, Miranda, P., & Victor, L. M. (1992). Maximum entropy analysis of Portuguese tsunami data: The tsunamis of 28.02.1969 and 25.05.1975. *Science of Tsunami Hazards*, 9–20.

Baptista, M A, Miranda, P. M. A., Miranda, J. M., & Victor, L. M. (1996). Rupture extent of the 1755 Lisbon earthquake inferred from numerical modeling of tsunami data. Physics and Chemistry of the Earth, 21(1–2), 65–70. https://doi.org/10.1016/S0079-1946(97)00011-6

Baptista, M A, Miranda, P. M. A., Miranda, J. M., & Victor, L. M. (1998). Constrains on the source of the 1755 Lisbon tsunami inferred from numerical modelling of historical data on the source of the 1755 Lisbon tsunami. *Journal of Geodynamics*, *25*(1–2), 159–174. https://doi.org/10.1016/S0264-3707(97)00020-3

Baptista, M A, Heitor, S., Miranda, J. M., Miranda, P., & Victor, L. M. (1998). The 1755 Lisbon tsunami; evaluation of the tsunami parameters. *Journal of Geodynamics*, *25*(1–2), 143–157. https://doi.org/10.1016/S0264-3707(97)00019-7

Baptista, M A, Miranda, J. M., Chierici, F., & Zitellini, N. (2003). New study of the 1755 earthquake source based on multi-channel seismic survey data and tsunami modeling. *Natural Hazards and Earth System Science*, *3*(5), 333–340. https://doi.org/10.5194/nhess-3-333-2003

Baptista, M A, Miranda, J. M., Omira, R., & Antunes, C. (2011). Potential inundation of Lisbon downtown by a 1755-like tsunami. *Natural Hazards and Earth System Science*, *11*(12), 3319–3326. https://doi.org/10.5194/nhess-11-3319-2011

Barkan, R., ten Brink, U. S., & Lin, J. (2009). Far field tsunami simulations of the 1755 Lisbon earthquake: Implications for tsunami hazard to the U.S. East Coast and the Caribbean. *Marine Geology*, *264*(1–2), 109–122. https://doi.org/10.1016/j.margeo.2008.10.010

Chow, V. T. (1959). *Open-channel hydraulics*. (McGraw-Hill, Ed.) (p. 680). New York, USA.

Costa, P J M, Andrade, C., Freitas, M. C., Oliveira, M. A., Lopes, V., Dawson, A. G., et al. (2012). A tsunami record in the sedimentary archive of the central Algarve coast, Portugal: Characterizing sediment, reconstructing sources and inundation paths. *The Holocene*, *22*(8), 899–914. https://doi.org/10.1177/0959683611434227

Costa, P J M, Andrade, C., Dawson, A. G., Mahaney, W. C., Freitas, M. C., Paris, R., & Taborda, R. (2012). Microtextural characteristics of quartz grains transported and deposited by tsunamis and storms. *Sedimentary Geology*, *275–276*, 55–69. https://doi.org/10.1016/j.sedgeo.2012.07.013

Costa, Pedro José Miranda, Costas, S., González-Villanueva, R., Oliveira, M. A., Roelvink, D., Andrade, C., et al. (2016). How did the AD 1755 tsunami impact on sand barriers across the southern coast of Portugal? *Geomorphology*, *268*, 296–311. https://doi.org/10.1016/j.geomorph.2016.06.019

Deltares, . (2016). *Delft3D-FLOW User Manual* . Delft, Netherlands: Deltares.

Fukao, Y. (1973). Thrust faulting at a lithospheric plate boundary the Portugal earthquake of 1969. *Earth and Planetary Science Letters*, *18*(2), 205–216. https://doi.org/10.1016/0012-821X(73)90058-7

Gjevik, B., Pedersen, G., Dybesland, E., Harbitz, C. B., Miranda, P. M. A., Baptista, M. A., et al. (1997). Modeling tsunamis from earthquake sources near Gorringe Bank southwest of Portugal. *Journal of Geophysical Research*, *102*(C13), 27931–27949. https://doi.org/10.1029/97JC02179

Gutscher, M. A. (2006). The great Lisbon earthquake and tsunami of 1755: lessons from the recent Sumatra earthquakes and possible link to Plato's Atlantis. *European Review*, *14*(2), 181–191.

Gutscher, M. A., Baptista, M. A., & Miranda, J. M. (2006). The Gibraltar Arc seismogenic zone (part 2): Constraints on a shallow east dipping fault plane source for the 1755 Lisbon earthquake provided by tsunami modeling and seismic intensity. *Tectonophysics*, *426*(1–2), 153–166. https://doi.org/10.1016/j.tecto.2006.02.025

La Selle, S. M., Lunghino, B. D., Jaffe, B. E., Gelfenbaum, G., & Costa, P. J. M. (2015). Hurricane Sandy Washover Deposits on Fire Island, NY. *U.S. Geological Survey Open-File Report*, *2017-2014.* https://pubs.er.usgs.gov/publication/ofr20171014, 25.

Lima, V. V., Miranda, J. M., Baptista, M. A., Catalão, J., Gonzalez, M., Otero, L., et al. (2010). Impact of a 1755-like tsunami in Huelva, Spain. *Natural Hazards and Earth System Science*, *10*(1), 139–148. https://doi.org/10.5194/nhess-10-139-2010

Luis, J.F. (2007). Mirone: A multi-purpose tool for exploring grid data. Computers and Geoscience, 33 (1), 31-41. https://doi.org/10.1016/j.cageo.2006.05.005.

Mansinha, L. & Smylie, D.E., (1971). The displacement field of inclined faults, Bulletin of the Seismological Society of America, 61, 1433–1440

Moreira, S., Costa, P. J. M., Andrade, C., Ponte Lira, C., Freitas, M. C., Oliveira, M. A., & Reichart, G.-J. (2017). High resolution geochemical and grain-size analysis of the AD 1755 tsunami deposit: Insights into the inland extent and inundation phases. *Marine Geology*, *390*, 94–105. https://doi.org/10.1016/j.margeo.2017.04.007

Okada, Y. (1985). Surface deformation due to shear and tensile faults in a half-space. *Bulletin of the Seismological Society of America*, *75*(4), 1135–1154.

Omira, R., Baptista, M. A., Matias, L., Miranda, J. M., Catita, C., Carrilho, F., & Toto, E. (2009). Design of a Sea-level Tsunami Detection Network for the Gulf of Cadiz. *Natural Hazards and Earth System Science*, *9*(4), 1327–1338. https://doi.org/10.5194/nhess-9-1327-2009

Omira, R., Baptista, M. A., & Miranda, J. M. (2011). Evaluating tsunami impact on the gulf of cadiz coast (northeast atlantic). *Pure and Applied Geophysics*, *168*(6–7), 1033–1043. https://doi.org/10.1007/s00024-010-0217-7

Ramalho, I., Omira, R., El Moussaoui, S., Baptista, M. A., & Zaghloul, M. N. (2018). Tsunami-induced morphological change – A model-based impact assessment of the 1755 tsunami in NE Atlantic from the Morocco coast. *Geomorphology*, *319*, 78–91. https://doi.org/10.1016/j.geomorph.2018.07.013

Santos, A., & Koshimura, S. (2015). The historical review of the 1755 lisbon tsunami. *Journal of Geodesy and Geomatics Engineering*, *2*(1). https://doi.org/10.17265/2332-8223/2015.04.004

Veloso, J. A. V. (2015). *Tremeu a Europa e o Brasil também* (1st ed., Vol. 1, p. 414). Brasil: Editora Chiado.

Vilanova, S. P., & Fonseca, J. F. B. D. (2004). Seismic hazard impact of the Lower Tagus Valley Fault Zone (SW Iberia). *Journal of Seismology*, *8*(3), 331–345. https://doi.org/10.1023/B:JOSE.0000038457.01879.b0Wronna, M., Omira, R., & Baptista, M. A. (2015). Deterministic approach for multiple-source tsunami hazard assessment for Sines, Portugal. *Natural Hazards and Earth System Science*, *15*(11), 2557–2568. https://doi.org/10.5194/nhess-15-2557-2015

List of Figures

Figure 1 – Top image - Modeled earthquake sources locations, Area of Interest (AOI - Salgados), Historical run-up and simulated water level locations sources. Lower image - Sediment cores (red points), virtual tide station, and AB/AC profiles localizations at the Salgados.

Figure 2 – Simulated maximum and minimum vertical highest wave on the area of interest using different earthquake sources.

Figure 3 - Modelled sediment volume (m^3) versus measured sediment volume (m^3) with varying Manning's roughness coefficient.

Figure 4 - Erosion and deposition thickness using Manning's roughness coefficient of 0.025 $m^{-1/3}s$ to all AOI. a) CAW, b) HSF, c) GB, d) MPF, e) Scenario 1, f) Scenario 2, g) Scenario 3

Figure 5 – A- GPR and modeled erosion and deposition thickness variation along profile AB (see Figure 1 for precise location) with 0.025 $m^{-1/3}s$ Manning's roughness coefficient. B - GPR and modeled erosion and deposition thickness variation along profile AC (see Figure 1 for precise location) with 0.025 $m^{-1/3}s$ Manning's roughness coefficient.

List of Tables

Table 1 – Fault parameters for the modeled hypothetical tectonic sources (Values obtained from averaging data provided in selected references (Gjevik et al., 1997; Baptista et al., 2003; Gutsher et al., 2006; Barkan et al., 2009; Omira et al. 2009; Lima et al. 2010; Omira et al. 2010; Baptista et al. 2011; Wronna et al. 2015; Ramalho et al. 2016; Silva 2017).

Comparison of tsunami travel time (TTT), in minutes, and run-up, in meters, at coastal locations along the broad Gulf of Cadiz retrieved from the historical record and yielded by modeling different epicentral areas.

Figure 1.

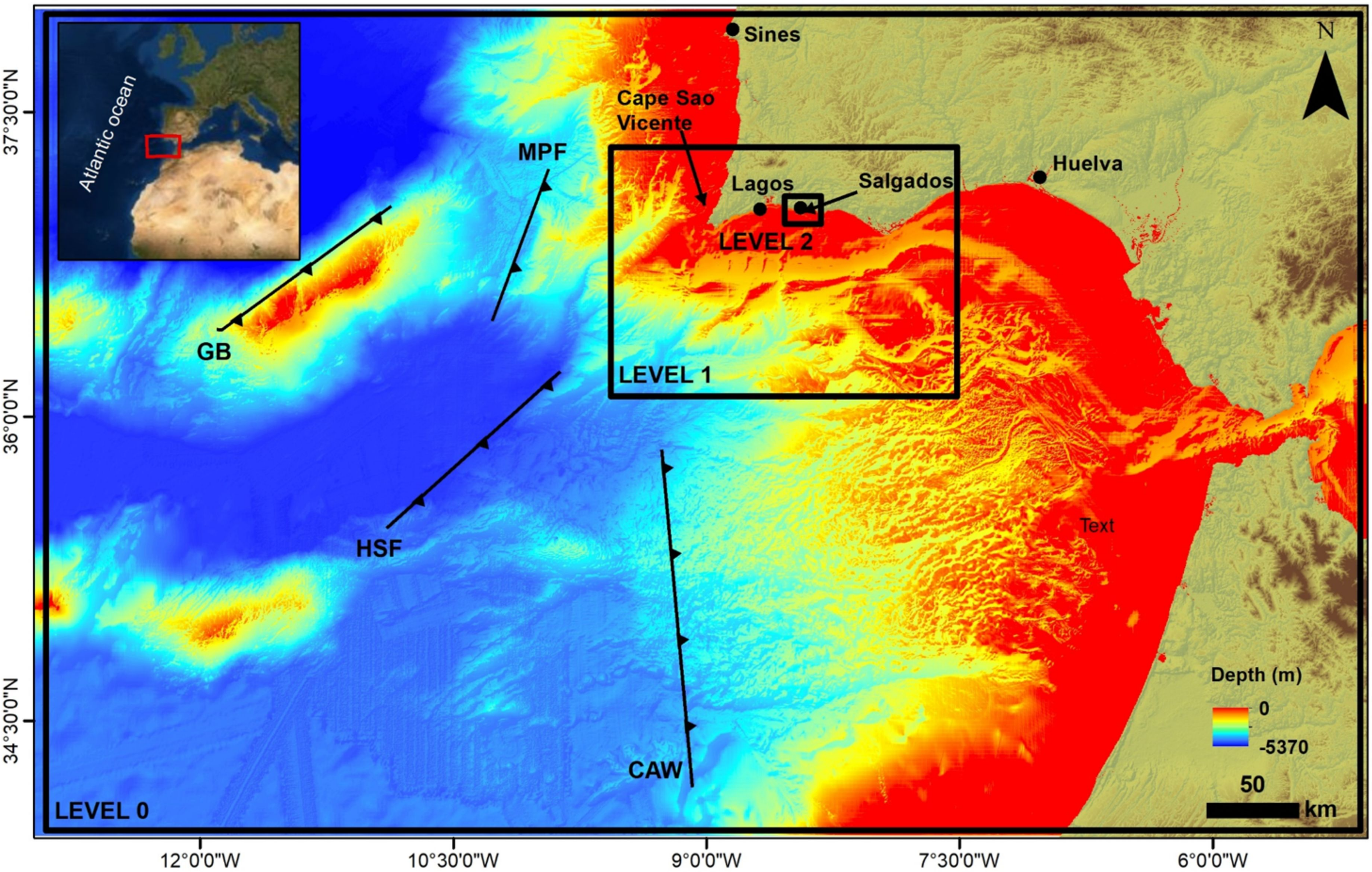

Atlantic ocean
Sines
Cape Sao Vicente
MPF
Lagos
Salgados
Huelva
LEVEL 2
GB
LEVEL 1
HSF
Text
CAW
Depth (m)
0
-5370
50
km
LEVEL 0
N
37°30'0"N
36°0'0"N
34°30'0"N
12°0'0"W
10°30'0"W
9°0'0"W
7°30'0"W
6°0'0"W

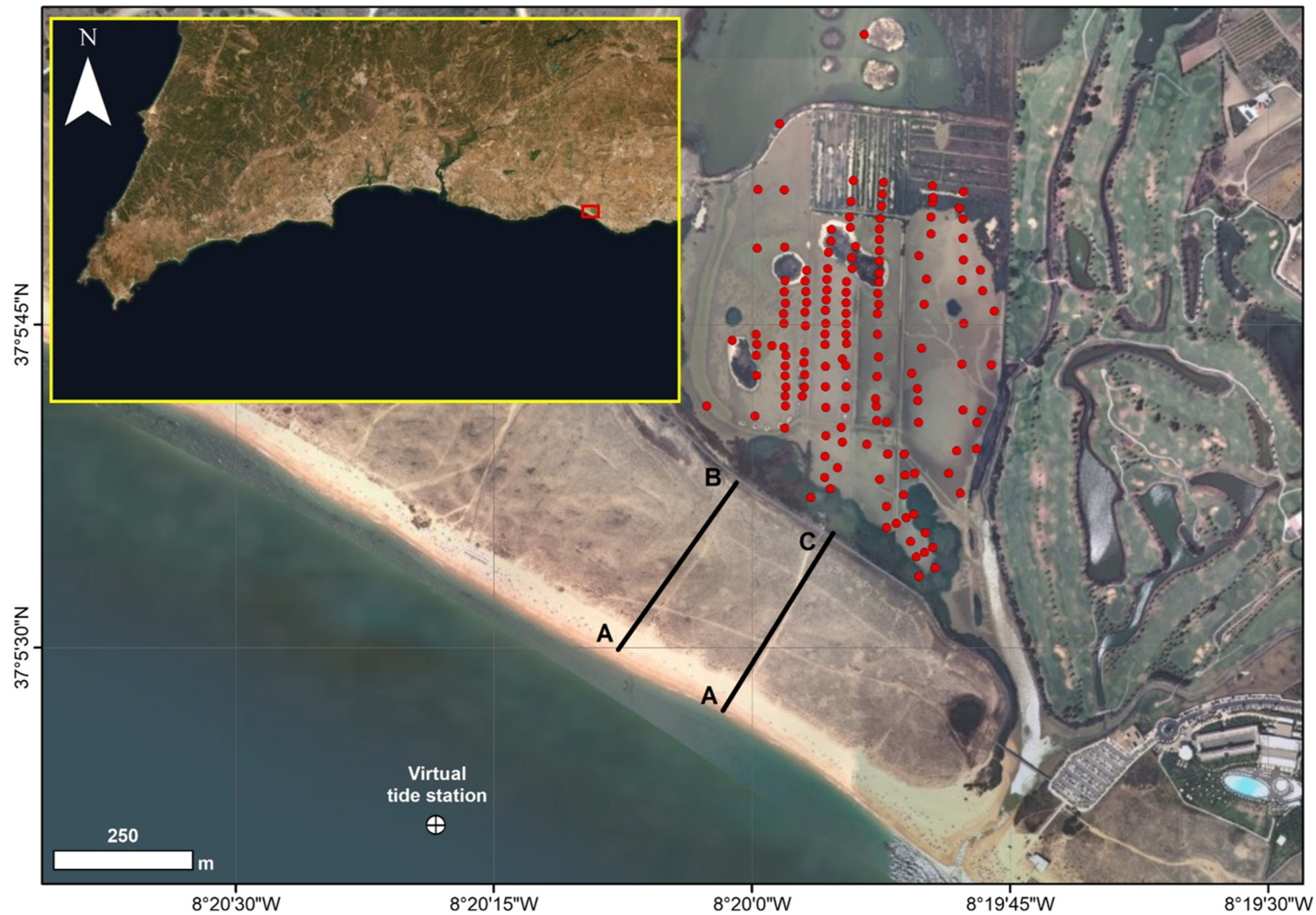

N
B
C
A
A
Virtual tide station
250
m
37°5'45"N
37°5'30"N
8°20'30"W
8°20'15"W
8°20'0"W
8°19'45"W
8°19'30"W

Figure 2.

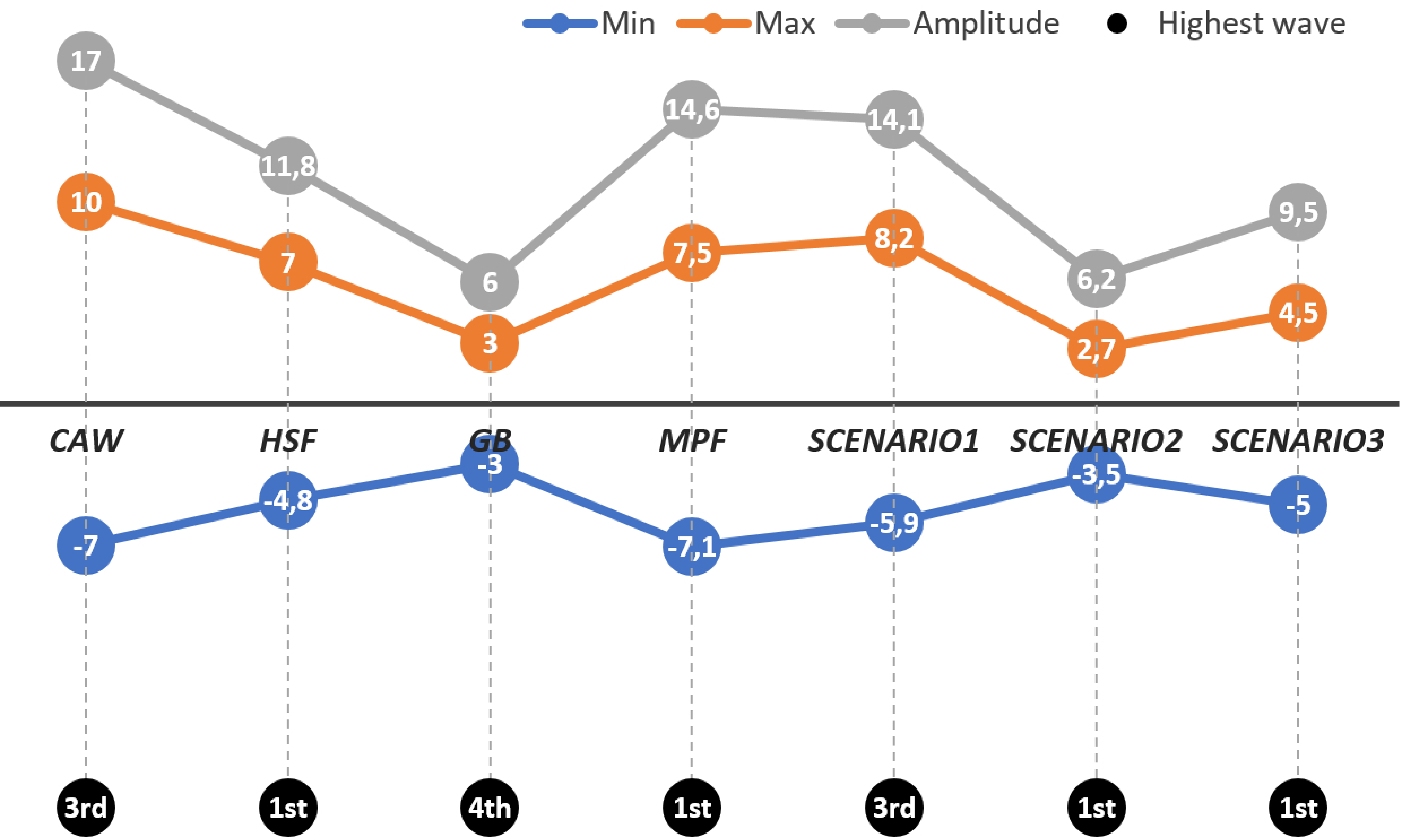

Min
Max
Amplitude
Highest wave
17
11,8
6
14,6
14,1
6,2
9,5
10
7
3
7,5
8,2
2,7
4,5
CAW
HSF
GB
MPF
SCENARIO1
SCENARIO2
SCENARIO3
-7
-4,8
-3
-7,1
-5,9
-3,5
-5
3rd
1st
4th
1st
3rd
1st
1st

Figure 3.

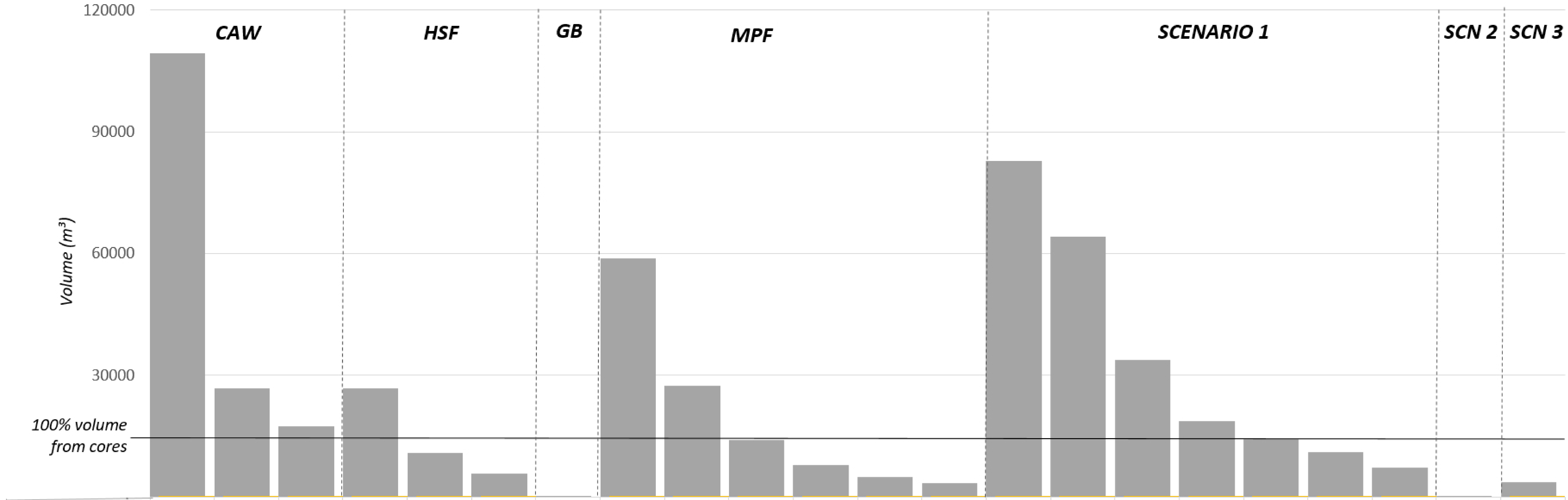

Roughness Coeficient	0.025	0,07	0,08	0.025	0,04	0,05	0.025	0.025	0,04	0,05	0,06	0,07	0,08	0.025	0,04	0,05	0,06	0,065	0,7	0,8	0.025	0.025
Vol. in m^3	109400	26800	17400	26700	10867	5831	159	58849	27301	14022	7830	4936	3403	82739	64182	33802	18620	14116	11078	7218	19	3550
% Vol. from cores	762%	187%	121%	186%	75,70%	40,60%	1,10%	410%	190%	97,70%	54,60%	34,40%	23,70%	576%	447%	235%	130%	98,40%	77,20%	50,30%	0,10%	24,70%

Figure 4.

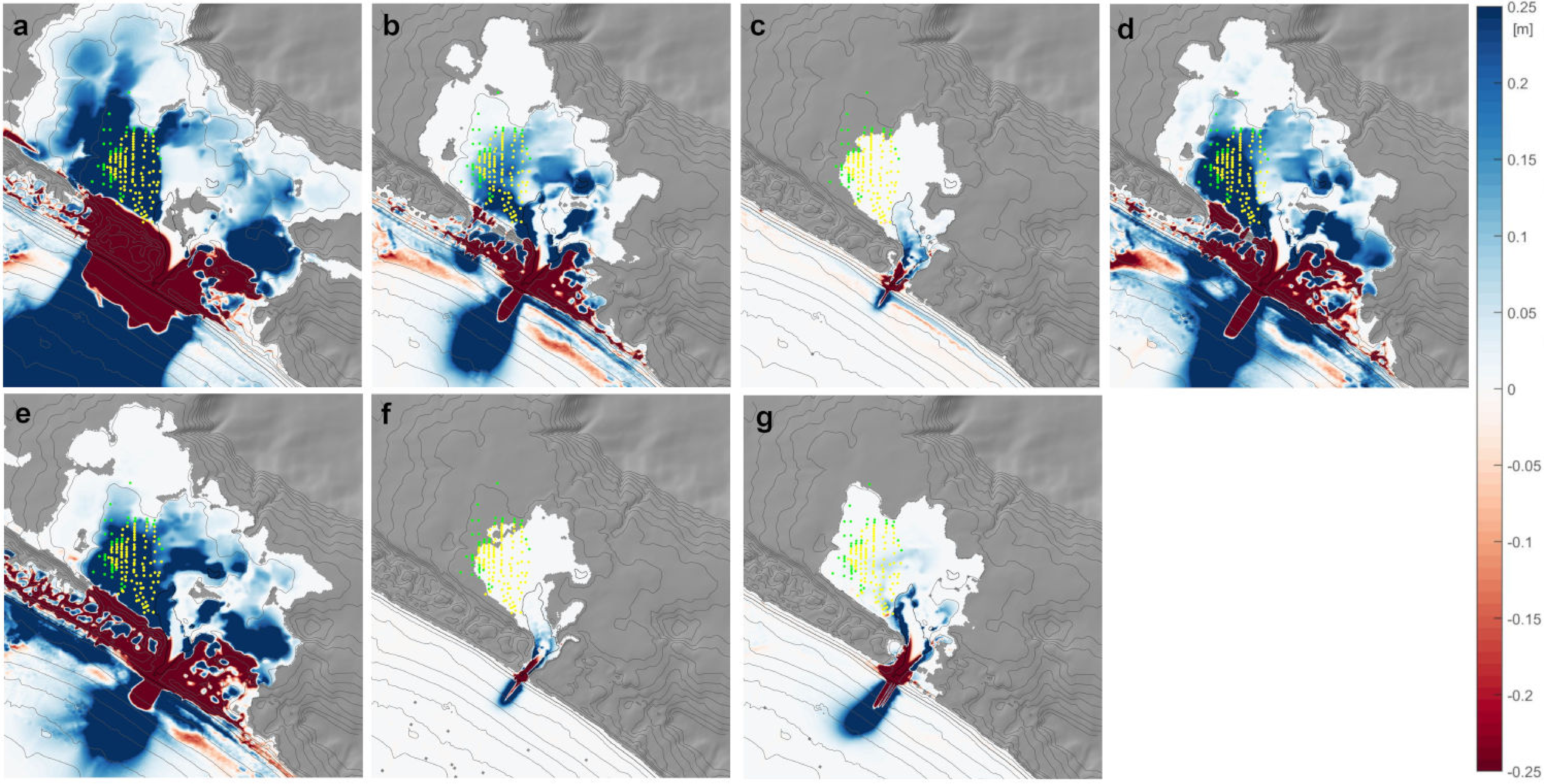

a
b
c
d
e
f
g
0.25
[m]
0.2
0.15
0.1
0.05
0
-0.05
-0.1
-0.15
-0.2
-0.25

Figure 5.

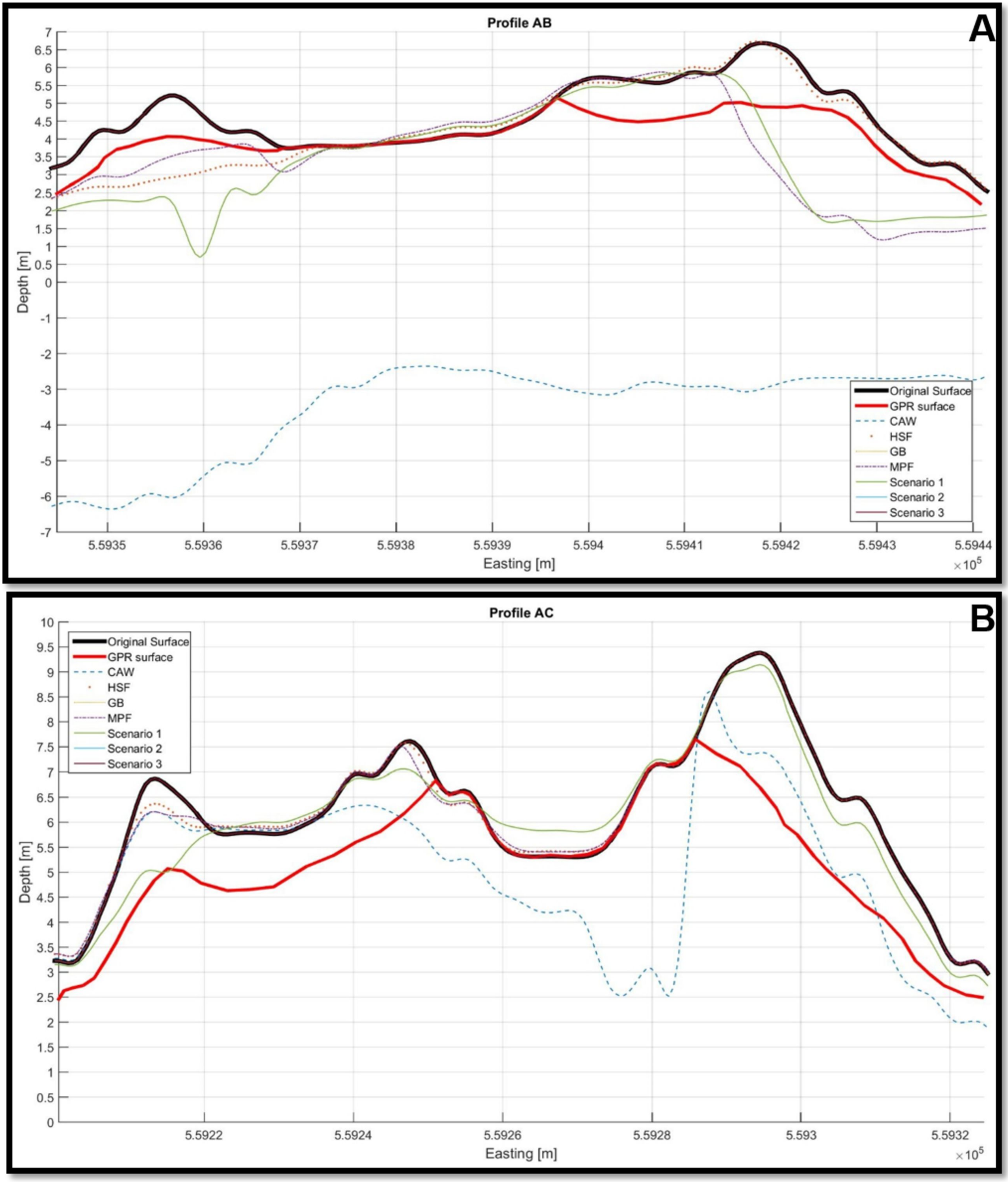

A
Profile AB
Depth [m]
Easting [m]
×10^5
Original Surface
GPR surface
CAW
HSF
GB
MPF
Scenario 1
Scenario 2
Scenario 3
B
Profile AC
Depth [m]
Easting [m]
×10^5
Original Surface
GPR surface
CAW
HSF
GB
MPF
Scenario 1
Scenario 2
Scenario 3

Table 1 – Fault parameters for the modeled hypothetical tectonic sources (Values obtained from averaging data provided in selected references (Gjevik et al., 1997; Baptista et al., 2003; Gutsher et al., 2006; Barkan et al., 2009; Omira et al. 2009; Lima et al. 2010; Omira et al. 2010; Baptista et al. 2011; Wronna et al. 2015; Ramalho et al. 2016; Silva 2017).
Comparison of tsunami travel time (TTT), in minutes, and run-up, in meters, at coastal locations along the broad Gulf of Cadiz retrieved from the historical record and yielded by modeling different epicentral areas.

Source	**CAW**	**HSF**	**GB**	**MPF**	**Scenario 1**	**Scenario 2**	**Scenario 3**
Depth (km)	5	5	5	5	5	60	60
Length (km)	120	114	120	110	114/120	127	127
Width (km)	60	100	60	70	60/70	170	300
Slip (m)	10	14	10	12	10/12	15	10
Strike (°)	57	42	57	23	42/57	52	52
Dip (°)	35	35	35	35	35	35	25
Rake (°)	90	90	90	90	90	90	90
Magnitude	8.8	8.4	8.2	8.2	8.4	8.6	8.6
Sines **Historical TTT** **(30 min)**	40	34	*34*	29	34	*28*	26
Sines **Historical Run-Up** **(no information)**	-	-	-	-	-	-	-
São Vicente **Historical TTT** **(16-17min)**	21	18	*25*	15	20	*18*	18
São Vicente **Historical Run-Up** **(11-15m)**	13	19	*8*	12	17	*5*	6
Lagos **Historical TTT** **(23-30 min)**	27	27	*39*	28	28	*31*	30
Lagos **Historical Run-Up** **(10 m)**	10	9	5	12	12	4	6
Huelva **Historical TTT** **(45-50 min)**	40	50	>60	50	55	>60	>60
Huelva **Historical Run-Up** **(No information)**	-	-	-	-	-	-	-